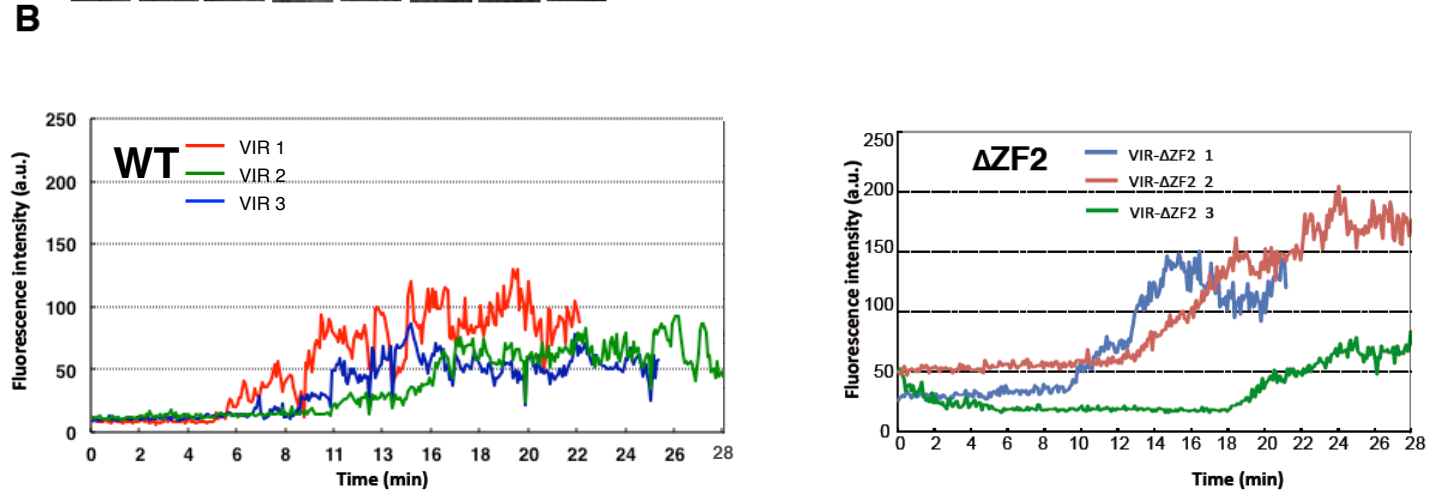
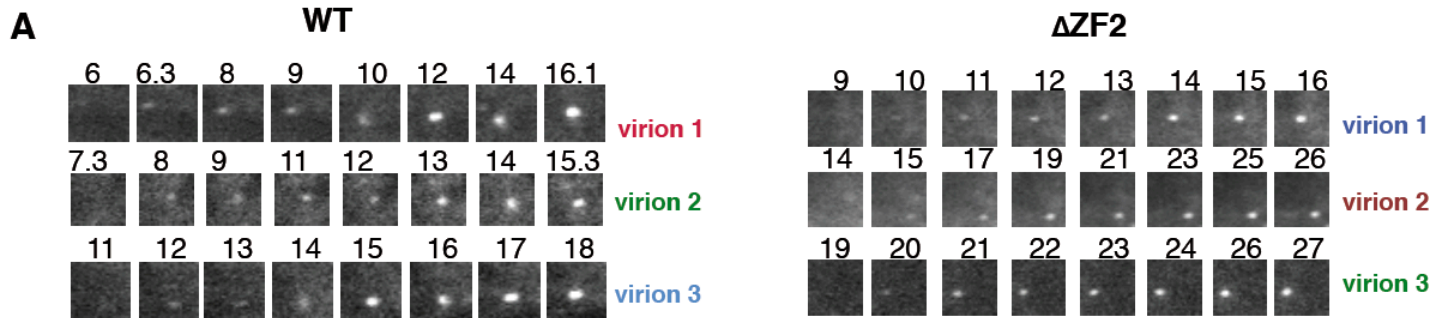


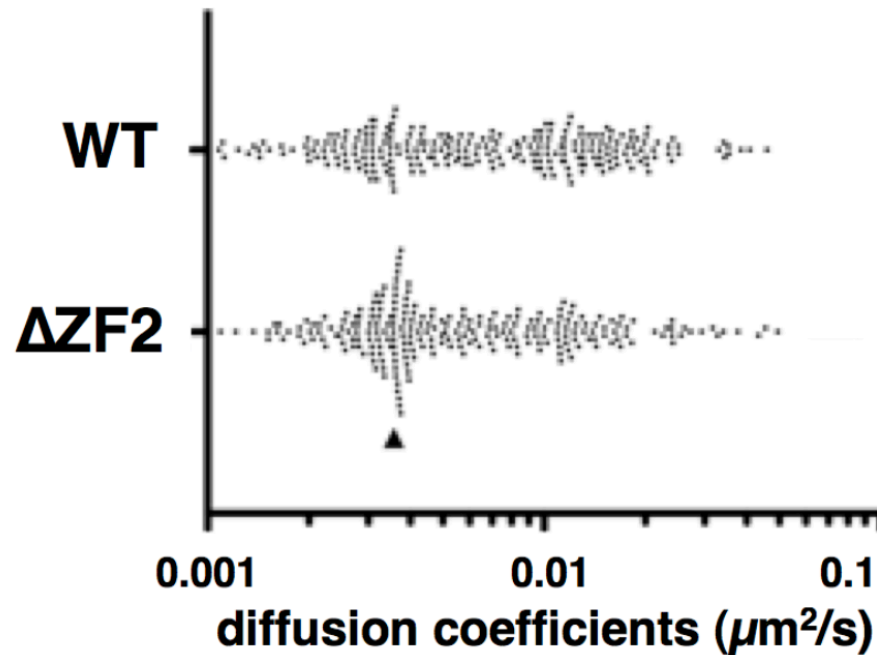
Supplemental Fig S1: Cartoons of HIV-1 and FV replication cycles with focus on RT timing and nucleic acid packaging. HIV-1 copies its gRNA into cDNA mostly during early steps of replication, while FV achieves its DNA synthesis at a large extent after pre-assembly steps. The cells transfected by and producing ΔZF2 particles are indicated, showing an enhanced late RTion process leading to increased viral cDNA packaging. Sequences of wt and mutant NC are given in top left panel.



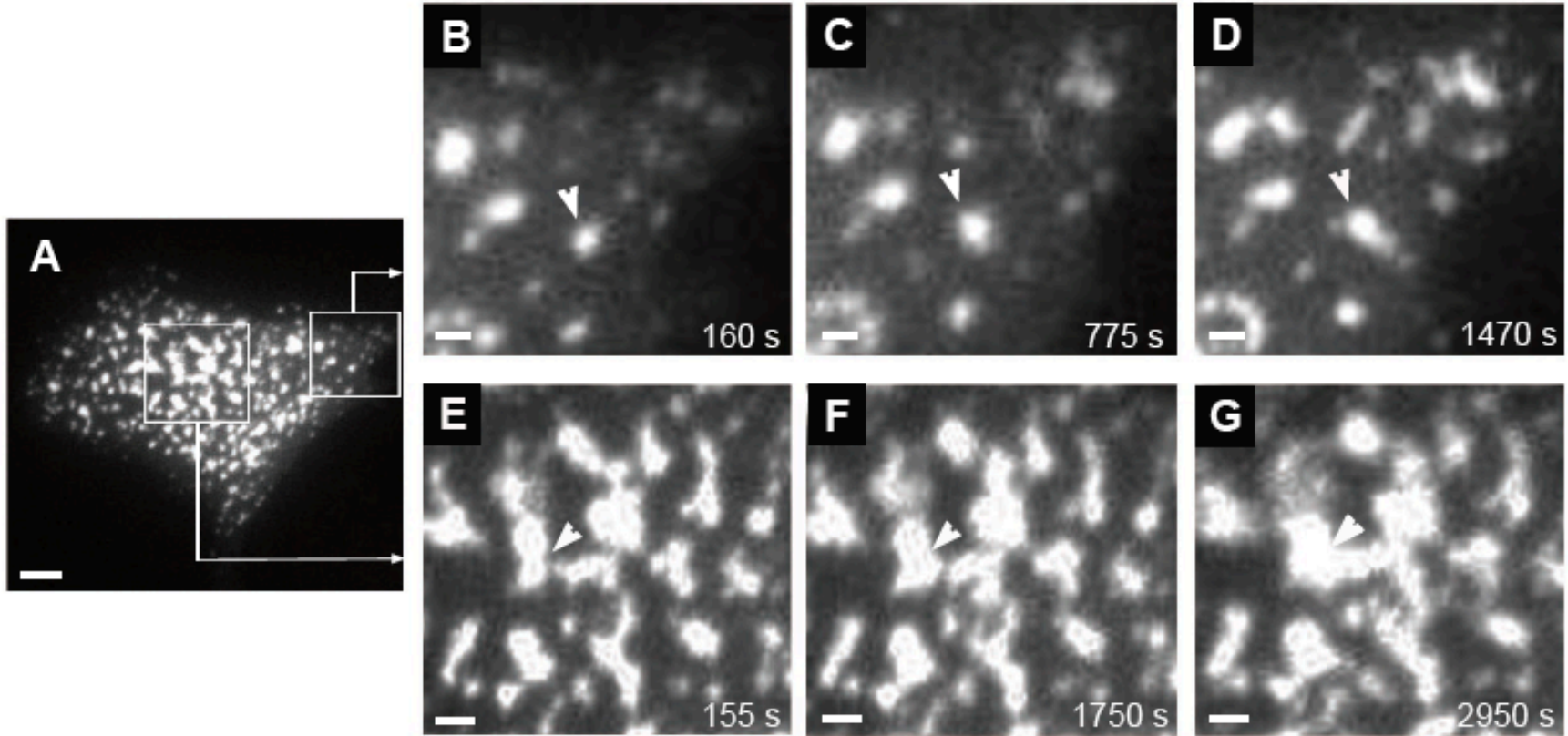
	events (n)	mean of time
WT	58	8 min 10 ± 0.3

	events (n)	mean of time
Δ ZF2	69	8 min 30 ± 0.4

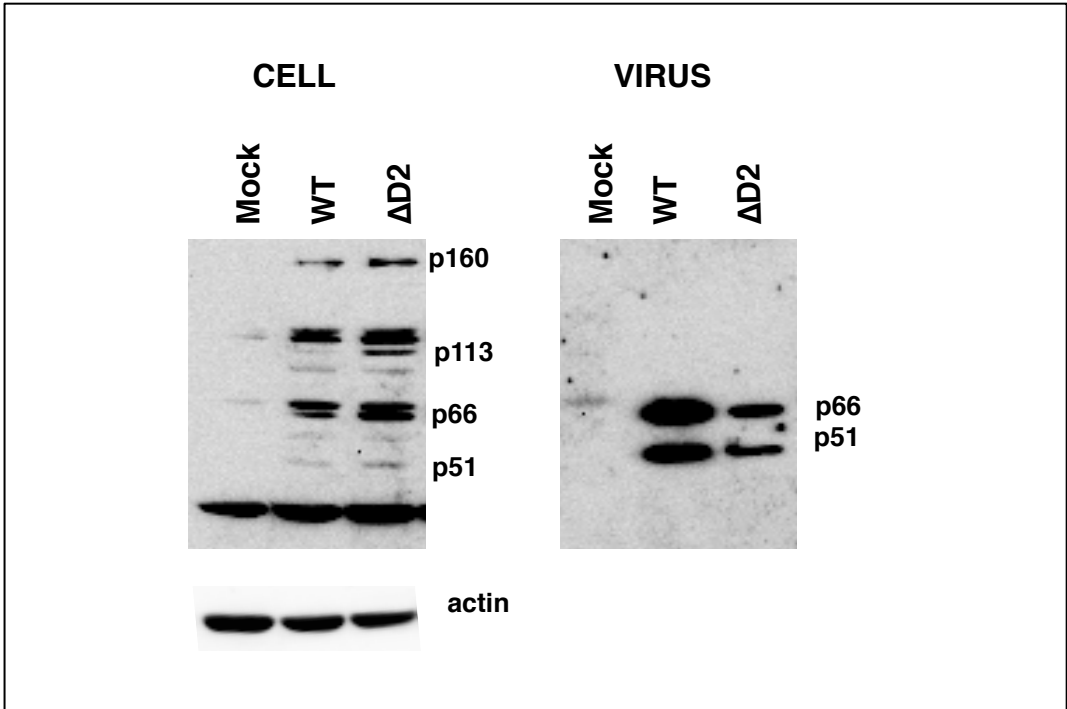
Supplemental Fig S2: Kinetics of Δ ZF2 HIV-1 assembly. HeLa cells were transfected 10-12 h with untagged and YFP-tagged Δ ZF2 HIV plasmids and imaged for 1-2 h at 1 frame/5 sec under TIRFM. (A) Images illustrate the formation of HIV-YFP puncta in the TIRF field corresponding to individual HIV-1 virion assembly events in HeLa cells. Images are $2.5 \times 2.5 \mu\text{m}^2$ and black numbers indicate the time of observation in minute. (B) Plots of fluorescence intensity in arbitrary units (a.u.) over time for the 3 assembly events shown in A. The time required to complete assembly was defined as the interval between the points of inflection on plots shown in B. Time was determined for >55 assembly events for both wt and Δ ZF2 HIV-1 and displayed as mean +/- SEM. p=0.7.



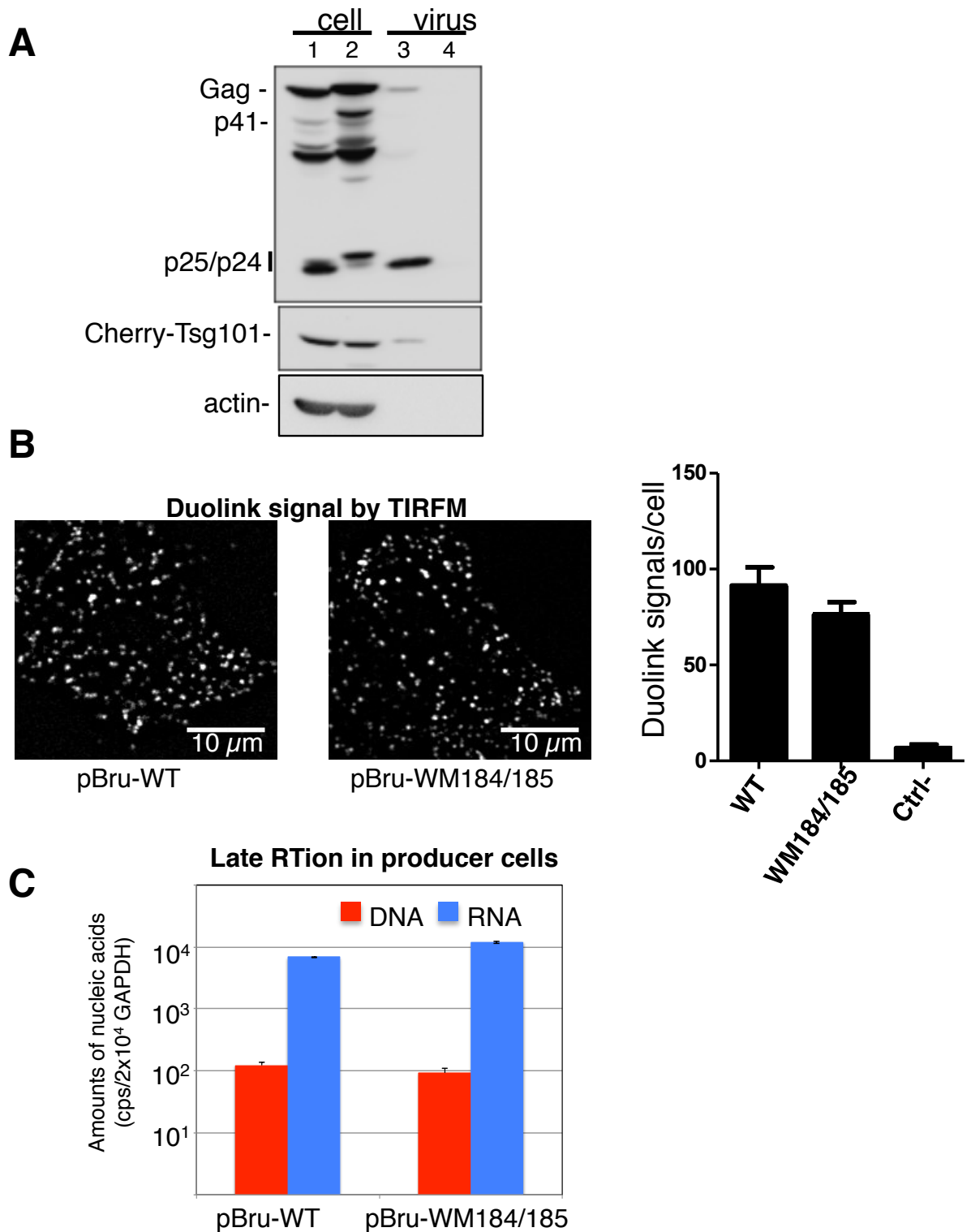
Supplemental Fig. S3: ΔZF2 particles exhibit reduced motility at the cell surface. Scatter plot of apparent diffusion coefficient calculated from individual viruses. Tracking was performed for individual particles in cells expressing HIV (250 particles, $n = 10$ cells). The black triangle highlights the increase of a population that was slowed down by the mutation.



Supplemental Fig. S4: Time lapse of the formation of large Gag-expressing area during Δ ZF2 HIV biogenesis at the PM of HeLa cells. Cells were transfected with untagged and YFP-tagged Δ ZF2 HIV plasmids and imaged at 14h post-transfection for 8 h with 1 frame/5 sec using TIRFM. A represents the entire cell producing Δ ZF2 HIV (same cell as in A). The 2 boxes correspond to the areas shown in the 2 time lapses. White arrowheads indicate the growth of domains. Time after the beginning of the observation is indicated in s in white (lower right). The upper panel highlights the growth of a patch from a nucleation point whereas the lower panel shows the fusion of two growing patches. Scale bars are 5 μ m (A) or 2 μ m (B to G).



Supplemental Fig S5: Representative Western blot images of Δ ZF2GagPol maturation in cells and virus. Cells were transfected with wt or Δ ZF2 pNL4-3 plasmid or an empty vector (mock) for 20 h. Proteins were extracted from cells and pelleted virus and were analyzed by Western blotting with an anti-HIV-1 RT (1/2000) or anti-actin (Sigma) as primary antibodies.



Supplemental Fig. S6: Effects of CA mutations (WM184/185) during virus biogenesis. HeLa cells were co-transfected with Tsg101-Cherry and pBru Δ env (WT or WM184/185) at the molar ratio 1:1. (A) Expression of Gag (WT:lanes 1-3; mutant: lanes 2-4) and Tsg101-Cherry in cells and virus release were analyzed by Western blotting using an anti-CA (top panel), anti-Cherry (middle panel) and anti-actin (bottom panel) as primary antibodies. (B) Duolink immunolabeling, TIRFM imaging and quantitation were performed as described in Fig. 2. (C) Nucleic acids were extracted from transfected cells and levels of gRNA and MS cDNA were determined as in Fig. 6.

Supplemental Text S7: Supplemental Experimental Procedures.

Plasmids

All HIV-1 plasmids in this study were based on pNL/HXB and were described elsewhere (1-3) with the exception of the pBRuWT Δ env and pBRuWM184/185 Δ env plasmids described in (4) (generous gift of J.R. Lingappa). HIV-1 pNL4-3 Δ ZF2 molecular clone was deleted of the entire ZF2 sequence as previously described (5). The HIV-1 proviral plasmid pL⁻ with the LTAL motif was previously described (6). The pNL4-3-derived proviral plasmid, pNL4-3-MA-YFP, that incorporated YFP into the stalk region of MA was previously described (7). The two plasmids, pNL4-3 Δ env and pNL4-3-MA-YFP Δ env, were deleted between the BglII₇₀₃₁-BglII₇₆₁₁ sites in the *env* gene. The two pCR3.1 SynGag Δ ZF2-YFP (or mCherry) and pCR3.1 SynGag Δ ZF2 were derived from the parental synGagWT plasmids described in (1) and mutant and WT versions were both used to visualize the genesis of VLP formed by Δ ZF2Gag or WTGag proteins alone. Vectors (pENX) used for *trans*-complementation assays were described in (6). pENX were deleted of p6, Pol, Vif and Vpr encoding sequences, using *Xho*I and *Sal*I (ENX Δ p6) and replaced with a synthetic oligonucleotide containing *Eco*RI, *Not*I and *Xho*I restriction sites. Thus, pENX-derived plasmid that express Tsg101 fused to the C terminus of a chimeric p6-deleted Gag protein (Gag^c), was generated by insertion of PCR product to generate Gag^c-Tsg101 (6). The Δ ZF2 version of all HIV-1 vectors was constructed by using QuickChange Lightning site-directed mutagenesis kit (Agilent). The pCR3.1-mCherry-Tsg101 plasmid was derived from pCR3.1-GFP-Tsg101 (8) in which GFP was substituted by mCherry by using *Hind*III and *Eco*RI sites. For the pulldown assays, PCR fragments encoding p15^{NCp1p6}, p9^{NCp1}, p7^{NC} or p6 domain were cloned into a donor vector (pDONR carrying two recombination sites attP) and then were inserted into pGex vector using the Gateway technology. The pNL4-3GagKO plasmid provides noncoding HIV gRNA which was knocked for translation by inserting a lacZ fragment (not in frame) after the Gag AUG.

Western blotting

For analysis of Gag or Tsg101 expression, cells were lysed in presence of protease inhibitor cocktail (Roche) with the ProteoJet reagent according to the manufacturer's instructions (Fermentas). Total protein concentration was determined by Bradford assay using a BSA standard set (Fermentas). Total proteins were loaded on 12% SDSPAGE and were transferred on blot. Gag was detected with anti-CA antibodies (1/150, H183 or 1/4000, Serotec) while endogenous Tsg101 and Cherry-Tsg101 were visualized with anti-Tsg101 (1/200, Santa Cruz) and anti-cherry (1/500, Chromotek) antibodies, respectively. Cellular actin was detected with an anti-actin (1/500, Sigma). After incubation with a peroxidase-conjugated (HRP) secondary antibody, ECL fluorescence was recorded by a CCD chemiluminescence camera system (Gnome, Syngene).

TIRF imaging

Cells plated on collagen-1 coated glass chambers were observed at 37°C with a homemade objective-type TIRF setup allowing multicolor single-molecule imaging and equipped with a Plan Fluor 100 \times /1.45 NA objective (Zeiss, Le Peck, France Brattleboro, VT) (9,10). All the experiments were carried out using a 100 ms integration time. In order to delimitate the areas at the cell membrane where Gag was present, the image obtained in the GFP channel was corrected for background (rolling radius of 100), Gaussian blurred (sigma radius=20) and automatically thresholded to create a selection representing the Gag-YFP signal (mainly localized at the PM). Only particles > 40 nm² were considered. Size of patches was calculated using Image J software after stacking frames of 10-15 s movies and normalization as compared to the background noise. Thousands of individual areas were measured and the areas for the samples under the different conditions were randomly uniformed to 300 using a list randomizer (random.org) and distributed in a scatter plot. The values in the results section are the average of the surface fluorescent areas \pm SEM with n equal to the number of experiments. Tracking was performed for individualized particles in cells using homemade software (named 'PaTrack') implemented in visual C++ (9). Briefly, trajectories were constructed using the individual diffraction limited signal of each small Gag cluster. The center of each fluorescence peak was determined with subpixel resolution by fitting a two-dimensional elliptical Gaussian function. The two-dimensional trajectories of clusters were constructed frame per frame. Diffusion coefficient values were determined from a linear fit to the MSD (mean square displacement)-t lag plots between the first and the fourth points (D_{1-4}) according to the equation $MSD(t) = 4Dt$.

Duolink assays

Gag-Tsg101 interaction was visualized *in situ* by using Duolink technique (11) that reveals whether two proteins might interact in the cell. HeLa cells were transfected with pCR3.1cherry-Tsg101 (0.2 μ g) and pNL4-3 Δ env (WT or Δ ZF2 or L-) at molar ratio of 0.2:1. After 20h cells were fixed for Duolink experiments. Proximity ligation assays were performed with anti-p17^{MA} (1/500) (AIDS Reagent Program) and anti-Tsg101 (1/25) (Santa Cruz) as primary antibodies (a control experiment was performed without anti-Tsg101). Then, immunostaining with Duolink kit was carried out following the

manufacturer's protocol (Sigma) with secondary antibodies conjugated to oligonucleotides that comprise one-half of a closed circle that can be ligated together only when the antibodies are in close proximity (< 40 nm). This complex can then be detected by rolling circle amplification with fluorescently tagged oligonucleotides. Cells were examined with a Nikon TE Eclipse TIRF microscope equipped with a 100x oil immersion objective and GFP filter, controlled by Metamorph software. Duolink signals were measured using Image J software as described in Figure 1 from 2 independent experiments. We chose n equal to the number of cells for SEM calculation. Total expression of Gag or Cherry-Tsg101 were monitored by anti-CA (H183) and anti-Cherry (Chromotek) Western blotting, respectively.

References

1. Jouvenet, N., Bieniasz, P.D. and Simon, S.M. (2008) Imaging the biogenesis of individual HIV-1 virions in live cells. *Nature*, **454**, 236-240.
2. Bieniasz, P.D. and Cullen, B.R. (2000) Multiple blocks to human immunodeficiency virus type 1 replication in rodent cells. *J Virol*, **74**, 9868-9877.
3. Jouvenet, N., Lainé, S., Pessel-Vivares, L. and Mougél, M. (2011) Cell biology of retroviral RNA packaging. *RNA Biology*, **8**, 1-9.
4. Klein, K.C., Reed, J.C., Tanaka, M., Nguyen, V.T., Giri, S. and Lingappa, J.R. (2011) HIV Gag-leucine zipper chimeras form ABCE1-containing intermediates and RNase-resistant immature capsids similar to those formed by wild-type HIV-1 Gag. *J Virol*, **85**, 7419-7435.
5. Grigorov, B., Decimo, D., Smagulova, F., Pechoux, C., Mougél, M., Muriaux, D. and Darlix, J.L. (2007) Intracellular HIV-1 Gag localization is impaired by mutations in the nucleocapsid zinc fingers. *Retrovirology*, **4**, 54.
6. Martin-Serrano, J., Zang, T. and Bieniasz, P.D. (2001) HIV-1 and Ebola virus encode small peptide motifs that recruit Tsg101 to sites of particle assembly to facilitate egress. *Nat Med*, **7**, 1313-1319.
7. Jouvenet, N., Neil, S.J., Bess, C., Johnson, M.C., Virgen, C.A., Simon, S.M. and Bieniasz, P.D. (2006) Plasma membrane is the site of productive HIV-1 particle assembly. *PLoS Biol*, **4**, e435.
8. Martin-Serrano, J. and Bieniasz, P.D. (2003) A bipartite late-budding domain in human immunodeficiency virus type 1. *J Virol*, **77**, 12373-12377.
9. Kremontsov, D.N., Rassam, P., Margeat, E., Roy, N.H., Schneider-Schaulies, J., Milhiet, P.E. and Thali, M. (2010) HIV-1 assembly differentially alters dynamics and partitioning of tetraspanins and raft components. *Traffic*, **11**, 1401-1414.
10. Espenel, C., Giocondi, M.C., Seantier, B., Dosset, P., Milhiet, P.E. and Le Grimellec, C. (2008) Temperature-dependent imaging of living cells by AFM. *Ultramicroscopy*, **108**, 1174-1180.
11. Gullberg, M., Göransson, C. and Fredriksson, S. (2011) Duolink-"In-cell Co-IP" for visualization of protein interactions in situ. *Nature Methods*, **8**.